

spherical particles. This is important since ultimately we want to be able to derive more reliable snow depth and snow water equivalent values using radiative transfer methods (snow algorithms). Initially, this problem will be addressed by modeling the scattering cross section (phase angles) for different snow crystal shapes and orientations at various incidence angles.

REFERENCES

- [1] R. Armstrong, A. Chang, A. Rango, and E. Josberger, "Snow depth and grain size relationships with relevance for passive microwave studies," *Ann. Glaciol.*, vol. 17, pp. 171–176, 1992.
- [2] A. T. C. Chang, P. Gloersen, T. Schmugge, T. Wilheit, and H. J. Zwally, "Microwave emission from snow and glacier ice," *J. Glaciol.*, vol. 16, pp. 23–39, 1976.
- [3] A. T. C. Chang, J. L. Foster, and D. K. Hall, "Nimbus-7 SMMR derived global snow cover parameters," *Ann. Glaciol.*, vol. 9, pp. 39–44, 1987.
- [4] B. Draine, "The discrete dipole approximation and its application to interstellar graphite grains," *J. Astrophys.*, vol. 33, pp. 848–872, 1988.
- [5] B. Draine and P. Flatau, "Discrete dipole approximation for scattering calculations," *J. Amer. Opt. Soc.*, vol. 11, pp. 1491–1499, 1994.
- [6] J. L. Foster, D. K. Chang, and A. T. C. Chang, "An overview of passive microwave snow research and results," *Rev. Geophys. Space Phys.*, vol. 1984, pp. 195–208.
- [7] J. Foster, D. Hall, A. Chang, A. Rango, W. Wergin, and E. Erbe, "Observations of snow crystal shape in cold snowpacks using scanning electron microscopy," in *Proc. Int. Geosci. Remote Sensing Symp.*, vol. 4, Lincoln, NE, 1996, pp. 2011–2013.
- [8] —, "Snow crystal shape and microwave scattering," in *Proc. Int. Geosci. Remote Sensing Symp.*, vol. 2, Singapore, 1997, pp. 625–627.
- [9] J. Foster, A. Chang, D. Hall, A. Rango, W. Wergin, and E. Erbe, "Effects of snow crystal shape on passive microwave radiation," *IEEE Trans. Geosci. Remote Sensing*, to be published.
- [10] J. Goodman, B. Draine, and P. Flatau, "Applications of FFT techniques to the discrete dipole approximation," *Opt. Lett.*, vol. 16, pp. 1198–1200, 1991.
- [11] D. K. Hall, A. T. C. Chang, and J. L. Foster, "Polarization responses to snow depth in the midwestern U.S.," *Nordic Hydrol.*, vol. 15, pp. 1–8, 1984.
- [12] M. Hallikainen, "Microwave radiometry of snow," *Adv. Space Res.*, vol. 9, no. 1, pp. 267–275, 1989.
- [13] D. Lynch and W. Livingston, *Color and Light in Nature*. Cambridge, U.K.: Cambridge Univ. Press, 1995, pp. 152–166.
- [14] C. Matzler, "Autocorrelation functions of granular media with arrangement of spheres, spherical shells or ellipsoids," *J. Appl. Phys.*, vol. 3, pp. 1509–1517, 1997.
- [15] N. Oreskes, K. Shrader-Frechette, and K. Belitz, "Verification, validation and confirmation of numerical models in the earth sciences," *Science*, vol. 23, pp. 762–767, 1994.
- [16] T. Schmugge, "Techniques and applications of microwave radiometry," in *Remote Sensing of Geology*, B. Siegal and A. Gillespie, Eds. New York: Wiley, 1980, ch. 11, pp. 337–352.
- [17] P. R. Siqueira, K. Sarabandi, and F. T. Ulaby, "Numerical simulation of scatterer positions in a very dense medium with an application to the two-dimensional Born approximation," *Radio Sci.*, vol. 30, no. 5, pp. 1325–1338, 1995.
- [18] F. T. Ulaby and W. H. Stiles, "The active and passive microwave response to snow parameters," *J. Geophys. Res.*, vol. 85, pp. 1045–1049, 1981.
- [19] F. T. Ulaby, K. Moore, and A. K. Fung, *Microwave Remote Sensing: Active and Passive*. Reading, MA: Addison-Wesley, 1986.
- [20] A. E. Walker and B. E. Goodison, "Discrimination of a wet snow cover using passive microwave satellite data," *Ann. Glaciol.*, vol. 17, pp. 307–311.

Estimates of Faraday Rotation With Passive Microwave Polarimetry for Microwave Remote Sensing of Earth Surfaces

Simon H. Yueh

Abstract—A technique based on microwave passive polarimetry for the estimates of ionospheric Faraday rotation for microwave remote sensing of Earth surfaces is described. Under the assumption of azimuth symmetry for the surfaces under investigation, it is possible to estimate the ionospheric Faraday rotation from the third Stokes parameter of microwave radiation. An error analysis shows that the Faraday rotation can be estimated with an accuracy of better than 1° with a space-based L-Band system, and the residual correction errors of linearly polarized brightness temperatures can be less than 0.1 K. It is suggested that the estimated Faraday rotation angle can be further utilized to derive the ionospheric total electron content (TEC) with an accuracy of about 1 TECU = 10^{16} electrons-m $^{-2}$, which will yield 1 mm accuracy for the estimate of an ionospheric differential delay at Ku-band. Therefore, this technique can potentially provide accurate estimates of ionospheric Faraday rotation, TEC, and differential path delay for applications including microwave radiometry and scatterometry of ocean salinity and soil moisture as well as satellite altimetry of sea surface height. A conceptual design applicable to real aperture and aperture synthesis radiometers is described for the measurements of the third Stokes parameter.

I. INTRODUCTION

Ocean surface salinity and soil moisture are crucial parameters for the modeling of surface hydrological processes. Global measurements of these two parameters require the deployment of spaceborne microwave sensors. Although L-Band microwave frequencies are found to be suitable for the remote sensing of ocean surface salinity and soil moisture [1]–[5], spaceborne measurements of L-Band microwave emission and radar backscatter from the Earth surfaces are subjective to the influence of ionospheric Faraday rotation. The radiometric errors in the linearly polarized brightness temperatures can be larger than 10 K for incidence angles in the range of 30° to 50° . This error will limit the usefulness of data from daytime satellite passes for soil moisture applications and is unacceptable for ocean surface salinity measurements, which require excellent radiometric accuracy [1], [2]. This article introduces a technique using the passive microwave polarimetry to provide accurate estimates of Faraday rotation angle for microwave remote sensing of Earth surfaces from space.

Passive microwave polarimetry is not a new concept [7], but it is beginning to receive significant interest for Earth remote sensing because of its applications for ocean surface wind velocity measurements with microwave frequencies in the range of 10–37 GHz [8]–[10]. Several techniques have been suggested for the measurements of the third and fourth Stokes parameters of microwave radiation, including the ferrite polarization gyrator [9], microwave polarization combiner [10], and digital correlators developed for radiometer aperture synthesis [12], [13]. The aircraft flights conducted in the 1980's and 1990's have demonstrated that polarimetric radiometer measurements can now be made with an accuracy of better than a few tenths of K for Earth surface measurements [8]–[11]. It is proposed in this article that the polarimetric microwave measurements at about 1 GHz will provide

Manuscript received June 28, 1999; revised February 7, 2000. This work was supported by the Jet Propulsion Laboratory (JPL), California Institute of Technology, Pasadena, CA and by the National Aeronautics and Space Administration (NASA), Washington, DC.

S. H. Yueh is with the Jet Propulsion Laboratory, California Institute of Technology, Pasadena, CA 91109 USA (e-mail: simon.yueh@jpl.nasa.gov).

Publisher Item Identifier S 0196-2892(00)06228-8.

accurate information of the ionospheric Faraday rotation, and hence a microwave instrumentation for accurate corrections of Faraday rotation is possible for space remote sensing of sea surface salinity and soil moisture.

In Section II, we describe the principle of polarimetric radiometry for the estimates of ionospheric Faraday rotation angle. Error estimates of this technique are described in Section III. Section IV discusses how to implement this technique for real aperture and synthetic aperture radiometers. Section V summarizes the results of this paper.

II. POLARIMETRIC RADIOMETRY

A. Stokes Parameter and Faraday Rotation

The electromagnetic waves emitted from natural media are in general partially polarized. To fully characterize the polarization state of partially polarized thermal radiation, four parameters I , Q , U , and V were introduced by Sir George Stokes [7]. These four parameters are related to the horizontally and vertically polarized components of electric fields (E_h and E_v) by the following equation:

$$I_s = \begin{bmatrix} I \\ Q \\ U \\ V \end{bmatrix} = \frac{1}{2\eta} \begin{bmatrix} \langle |E_v|^2 \rangle + \langle |E_h|^2 \rangle \\ \langle |E_v|^2 \rangle - \langle |E_h|^2 \rangle \\ 2 \operatorname{Re} \langle E_v E_h^* \rangle \\ 2 \operatorname{Im} \langle E_v E_h^* \rangle \end{bmatrix}. \quad (1)$$

Here, the angular brackets denote the ensemble average of the argument, and η is the electromagnetic wave impedance [18]. The first Stokes parameter (I) represents the total radiated power density, and the second Stokes parameter (Q) is the difference of the power density in the vertical and horizontal polarization channels. The third and fourth Stokes parameters U and V characterize the correlation between these two linear polarizations.

Conventional radiometers for Earth remote sensing perform measurements of T_v and T_h , which are the brightness temperatures of vertical and horizontal polarizations. For convenience, we ignore a proportional constant that relates the power density to the brightness temperatures [18]. Hence, we can express T_v and T_h as

$$T_v = (I + Q)/2 \quad (2)$$

$$T_h = (I - Q)/2. \quad (3)$$

As the microwave radiation from the Earth surface propagates through the ionosphere, the linearly polarized field components are rotated by an angle Ω (Faraday rotation), depending on the geomagnetic field and ionospheric electron content. It may be expressed approximately as [6]

$$\Omega = 1.355 \times 10^4 f^{-2} N_f \langle B_0 \cos \alpha \sec \chi \rangle \quad (4)$$

where

- Ω in degrees;
- f radio frequency in GHz;
- N_f ionospheric total electron content (TEC) in TEC units;
- 1 TECU 10^{16} electrons \cdot m $^{-2}$;
- B_0 Earth magnetic field in Tesla;
- α angle between the magnetic field and wave propagation direction;
- χ angle between the wave propagation direction and the vertical to the surface.

The angular brackets denote an average of the enclosed quantities along the path of wave propagation. The intent of this equation is to provide an estimate of the Faraday rotation. If it is to be used to deduce the TEC

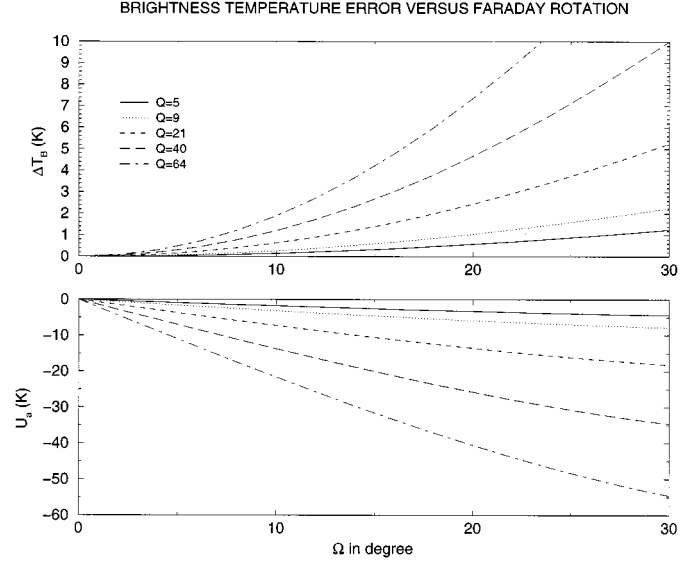


Fig. 1. Effects of Faraday rotation on the Stokes parameters of microwave radiation from Earth surfaces. The upper panel plots the change of horizontally polarized brightness temperatures for five different values of Q versus the Faraday rotation angle. The bottom panel plots the third Stokes parameter resulting from the Faraday rotation.

TABLE I
SEA SURFACE BRIGHTNESS TEMPERATURES AT 1.4 GHz PREDICTED BY A POLARIMETRIC TWO-SCALE SCATTERING MODEL [19] AT 10 m \cdot s $^{-1}$ WIND SPEED AND 45° AZIMUTH ANGLE RELATIVE TO THE WIND DIRECTION

Incidence Angle (degree)	T_v (K)	T_h (K)	Q (K)	U (K)
10	95.1	92.9	2.2	-0.12
15	96.6	91.5	5.1	-0.11
20	98.6	89.7	9.0	-0.11
30	105.1	84.4	20.7	-0.11
40	115.2	77.0	38.2	-0.10
50	130.4	67.6	62.8	-0.09

from the Faraday rotation, its accuracy influences the accuracy of the estimate.

N_f is significantly affected by the solar radiation. The TEC measurements performed by a network of GPS receivers [17] have shown significant temporal and spatial variations. In the equatorial and mid-latitude areas, N_f varies from a few TECU at night to as high as 60 TECU at noon, while N_f has less temporal variation with a nominal value of about 20 TECU in the polar regions. By assuming a typical worst-case geometry ($\chi = 45^\circ$, $\alpha = 0^\circ$), and a high-latitude value of $B_0 = 5.44 \times 10^{-5}$ at 300 km altitude near the peak of the electron density, an upper bound estimate for Ω in degrees at 1.4 GHz for a satellite operating above the ionosphere is

$$\Omega = 0.53 N_f. \quad (5)$$

Therefore, the Faraday rotation at a frequency of 1.4 GHz can be as low as a few degrees at night and as high as 20 to 30° at noon local time.

Let us denote the vertically and horizontally polarized components of the electric fields received by the satellite antenna by E_{va} and E_{ha} , the linearly polarized fields after propagating through the ionosphere. E_{va} and E_{ha} will be related to E_v and E_h by

$$E_{va} = E_v \cos \Omega + E_h \sin \Omega \quad (6)$$

$$E_{ha} = -E_v \sin \Omega + E_h \cos \Omega \quad (7)$$

From the above equations, it is straightforward to show that the Stokes parameters measured by the satellite antenna are related to those emitted from the surface by

$$I_a = I \quad (8)$$

$$Q_a = Q \cos 2\Omega + U \sin 2\Omega \quad (9)$$

$$U_a = -Q \sin 2\Omega + U \cos 2\Omega \quad (10)$$

$$V_a = V. \quad (11)$$

Here, the subscript a indicates the satellite measurements. The first and fourth Stokes parameters are insensitive to the Faraday rotation, but the second and third Stokes parameters are. It is also straightforward to show that

$$T_{va} = T_v - \Delta T_B \quad (12)$$

$$T_{ha} = T_h + \Delta T_B \quad (13)$$

where

$$\Delta T_B = Q \sin^2 \Omega - \frac{U}{2} \sin 2\Omega. \quad (14)$$

ΔT_B represents the effects introduced by the Faraday rotation.

If the Faraday rotation angle Ω is known, the Stokes parameters of the surface radiation can be inverted from the satellite measurements by

$$T_v = T_{va} - Q_a \sin^2 \Omega - \frac{U_a}{2} \sin 2\Omega \quad (15)$$

$$T_h = T_{ha} + Q_a \sin^2 \Omega + \frac{U_a}{2} \sin 2\Omega \quad (16)$$

$$Q = Q_a \cos 2\Omega - U_a \sin 2\Omega \quad (17)$$

$$U = U_a \cos 2\Omega + Q_a \sin 2\Omega. \quad (18)$$

Fig. 1 illustrates the effects of Faraday rotation on the horizontally polarized brightness temperature and the third Stokes parameter for several values of Q . The range of Q approximately corresponds to the ocean radiation at 1.4 GHz shown in Table I. ΔT_B can reach above 10 K at high incidence angles (high Q values) and can be lower than 1 K at near nadir angles (low Q values). The third Stokes parameter is shown to be highly sensitive to the Faraday rotation and can reach as high as about 30 to 50 K. Note that the results illustrated are applicable to land surfaces with similar Q values.

B. Azimuthal Symmetry and Estimates of Faraday Rotation

If the surfaces are azimuthally symmetric with no preferred direction of orientation, the third Stokes parameter U is zero [16]. There are nonazimuthally symmetric surfaces, such as plow fields and ocean surfaces, which have a preferred direction of corrugation. For plow fields, we are not aware of any measurements for the third Stokes parameter made at L-Band. For sea surfaces, however, the flight experiments by [8], [15] indicate that the third Stokes parameter U of sea surfaces is no more than a few tenths of K at L-Band frequencies. Table I provides the theoretical predictions of Stokes parameters for sea surfaces at 1.4 GHz with a two-scale scattering model [19] for 10 m·s⁻¹ winds at an azimuthal angle of 45° relative to the wind direction. The theoretical predictions for U at near nadir incidence angles agree excellently well with the data shown in [8], [15]. The data [8], [15] and theory suggest that the directional dependence of U of sea surfaces is less than about 0.1 K. In addition, U is shown to be much weaker than Q for above 15° incidence angles and hence, we can ignore the contributions of U to U_a for off-nadir observations of ocean surfaces.

Under the assumption of azimuthal asymmetry or ignoring the contribution of U , we obtain

$$Q_a = Q \cos 2\Omega \quad (19)$$

$$U_a = -Q \sin 2\Omega. \quad (20)$$

For ocean and most terrain surfaces, Q is greater than zero because the vertically polarized radiation has a better transmissivity through the surface than the horizontally polarized radiation due to the presence of Brewster angle for vertical polarization [18]. This allows us to solve for Ω and Q from the above equations

$$Q = \sqrt{Q_a^2 + U_a^2} \quad (21)$$

$$\tan 2\Omega = -\frac{U_a}{T_{va} - T_{ha}}. \quad (22)$$

Note that the above equations permit ambiguous solutions of Ω with integer multiples of 180°, but this is not a problem because all the ambiguities produce the same corrections for brightness temperatures. In practice, Ω is always less than 180° at L-Band microwave frequencies. The remaining uncertainties are the initial polarization angle due to the nature of the detected surface and measurement errors contributed by the microwave system.

Presently, there are no easy methods to measure TEC over oceans except in the areas near land, where there are GPS receivers deployed for TEC observations. The technique suggested here could fill a gap in ionospheric measurements.

III. ERROR ANALYSIS

The accuracy of the above algorithm is limited by the instrument measurement errors and the departure of the surfaces from azimuthal symmetry. If we represent the above errors by a quantity ΔU , the retrieved Q and Ω will be

$$Q' = \sqrt{Q_a^2 + (U_a + \Delta U)^2} \quad (23)$$

$$\tan 2\Omega' = -\frac{U_a + \Delta U}{T_{va} - T_{ha}}. \quad (24)$$

Fig. 2 plots the error ($\Delta\Omega = \Omega' - \Omega$) of the Faraday rotation angle estimated from the third Stokes parameter. The upper panel illustrates the error versus Ω for a fixed $Q = 40$ K and a range of ΔU . It is shown that the accuracy of Ω' can be better than 0.2° for $\Delta U \leq 0.2$ K. The bottom panel plots the accuracy of Ω' for a fixed value of $\Delta U = 0.2$ K. A larger second Stokes parameter Q clearly produces a more accurate estimate of Ω . This is expected because U is more sensitive to the Faraday rotation for larger Q .

If the estimated Faraday rotation angle Ω' is used to make corrections of the brightness temperature, the residual error in the horizontally polarized brightness temperature is illustrated in Fig. 3. The upper panel indicates that the residual error increases with Ω and is less than 0.1 K for $\Delta U = 0.2$ K at up to 30° Faraday rotation angle.

The lower panel in Fig. 3 plotting the residual error versus Q demonstrates that the accuracy of the brightness temperature corrections is fairly insensitive to the second Stokes parameter. This can be understood by examining (23) and (24). If we assume that Q is much greater than ΔU , Q' can be approximated by

$$Q' \approx Q - \Delta U \sin 2\Omega. \quad (25)$$

Therefore, the errors of the retrieved brightness temperatures will be

$$\Delta T_h = T'_h - T_h = -(T'_v - T_v) \approx \frac{\Delta U \sin 2\Omega}{2}. \quad (26)$$

Here, T'_v and T'_h are the corrected brightness temperatures. It appears that the residual brightness temperature errors are proportional to ΔU

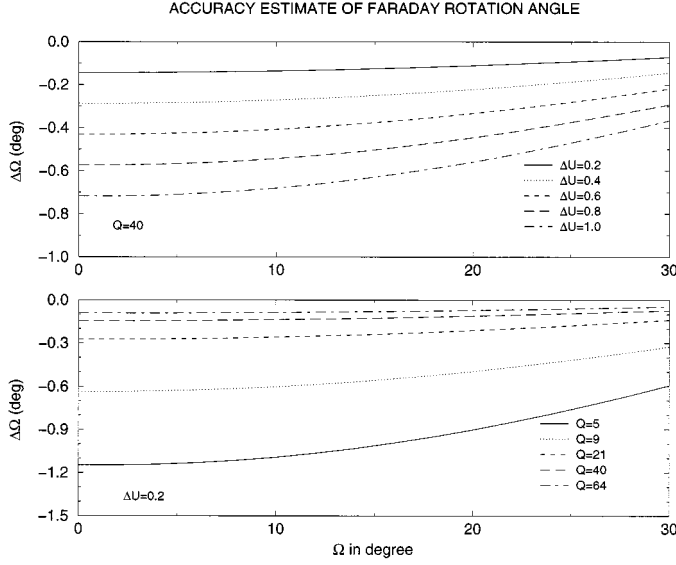


Fig. 2. Accuracy of the Faraday rotation angle estimated from the third Stokes parameter measurements. The upper illustrates the accuracy for $Q = 40$ K and five different ΔU values. The lower panel plots the errors for $\Delta U = 0.2$ K and five different values of Q .

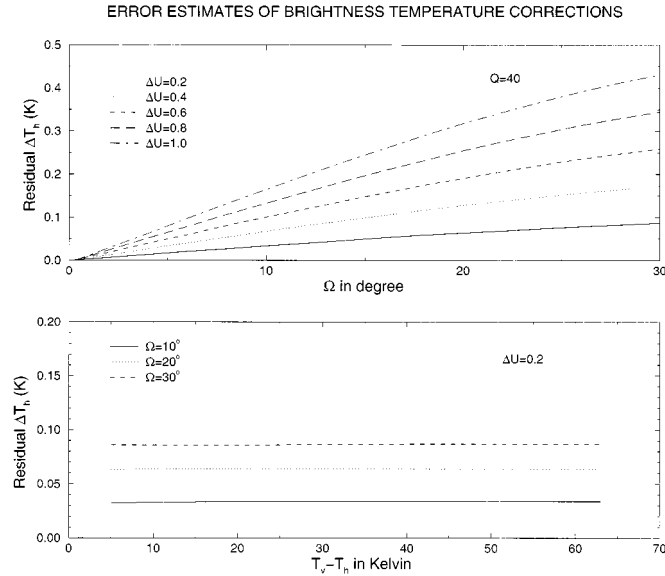


Fig. 3. Estimated accuracy of brightness temperatures corrected with the Faraday rotation angle estimated from the third Stokes parameter measurements. The upper illustrates the residual error of T_h for $Q = 40$ K which approximately corresponds to the sea surface radiation at 40° incidence and 1.4 GHz. The lower panel plots the residual errors versus Q for $\Delta U = 0.2$ K and three different values of Ω .

and are insensitive to Q . This implies that the accuracy of using the third Stokes parameter for brightness temperature corrections is limited by the measurement and modeling accuracy of U . Furthermore, because Q is related to the terrain types, a small sensitivity to Q suggests that this technique could provide a uniform brightness temperature correction for a large range of surface conditions.

The estimates of Faraday rotation angle can also be used to infer the ionospheric TEC through (4) and consequently the ionospheric differential delay. Equation (5) suggests that N_f can be estimated with an accuracy of about 0.5 TECU for $\Delta\Omega = 0.2^\circ$ and $f = 1.4$ GHz. Therefore, a space-based L-Band polarimetric radiometer can potentially provide global ionospheric TEC measurements with an accuracy

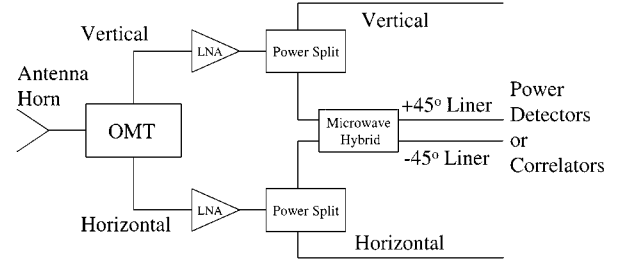


Fig. 4. Conceptual design for Stokes parameter measurements applicable to real aperture and aperture synthesis radiometers.

of about 1 TECU. Based on the relationship of ionospheric TEC and path delay described in [17], 1 TECU produces about 0.35 ns (10.5 cm one-way) differential delay at L-Band. Because the ionospheric differential delay is proportional to $1/f^2$, the accuracy will approach 3.5 ps (1 mm one-way) at Ku-band (14 GHz). This suggests that this technique could provide accurate estimates of ionospheric differential delay for sea surface height measurements with spaceborne altimeters.

IV. CONCEPTUAL DESIGN

A conceptual design (Fig. 4) for the measurement of the third Stokes parameter is proposed. This design is applicable to both real aperture and aperture synthesis radiometers. In this design, the surface radiation from the antenna is split into vertical and horizontal polarizations by the ortho-mode transducer (OMT). The signals from both polarization channels are amplified and then split into two channels for each polarization. A microwave-hybrid then adds and subtracts the vertically and horizontally polarized signals to produce $\pm 45^\circ$ linear polarizations.

For real-aperture radiometers, the power of signals from the vertical, horizontal, 45° -linear and -45° linear polarizations is detected to obtain T_v , T_h , T_{45} and T_{-45} , respectively. The third Stokes parameter U can be derived from any one of the following equations:

$$U = T_{45} - T_{-45} \quad (27)$$

$$U = 2T_{45} - T_v - T_h \quad (28)$$

$$U = T_v + T_h - 2T_{-45} \quad (29)$$

These equations have been implemented and tested for the Jet Propulsion Laboratory (JPL), Pasadena, CA, aircraft polarimetric radiometers [10]. The second and third equations require either T_{45} or T_{-45} measurements to produce the third Stokes parameter, and hence can probably simplify the design of the microwave hybrid and uses only three power detectors, instead of four.

The design indicated above is also applicable to aperture-synthesis radiometers [12]–[14], which take the output from a distributed set of antennas and correlate the signals to form the image. For this type of radiometer, the microwave scheme proposed here has to be implemented for each antenna and associated frontend receiver. The backend correlators can then switch between these polarization channels to form the images of T_v , T_h , T_{45} , and T_{-45} . The third Stokes parameter for each pixel in the image can then be synthesized from the equations described above.

V. SUMMARY

This article suggests the use of polarimetric passive microwave measurements for the estimates of ionospheric Faraday rotation. Applications can be considered for microwave radiometry of ocean surface salinity and soil moisture and altimetry of sea surface height. The analysis shows that this technique can provide accurate estimates of Faraday rotation angle and is effective for the corrections of

radiometric errors due to Faraday rotation. With measurement errors for the third Stokes parameter in the order of 0.1–0.2 K, it is shown that the residual errors in the corrected brightness temperatures can be reduced to less than 0.1 K. This makes it feasible to use low-frequency microwave waves to remotely sense ocean salinity and soil moisture from space for both daytime and nighttime satellite passes. A conceptual design for hardware implementation is described and is applicable to both real-aperture and aperture-synthesis radiometers.

REFERENCES

- [1] C. T. Swift and R. E. McIntosh, "Considerations for microwave remote sensing of ocean surface salinity," *IEEE Trans. Geosci. Remote Sensing*, vol. GE-21, pp. 480–491, July 1983.
- [2] G. Lagerloef, C. T. Swift, and D. LeVine, "Sea surface salinity: The next remote sensing challenge," *Oceanography*, vol. 8, pp. 44–50, 1995.
- [3] T. J. Jackson, D. M. LeVine, C. T. Swift, T. J. Schmugge, and F. R. Schiebe, "Large-area mapping of soil moisture using ESTAR passive microwave radiometry in Washita'92 experiment," *Remote Sens. Environ.*, vol. 53, pp. 23–37, 1995.
- [4] E. G. Njoku, Y. Rahmat-Samii, J. Sercel, W. J. Wilson, and M. Moghaddam, "Evaluation of an inflatable antenna concept for microwave sensing of soil moisture and ocean salinity," *IEEE Trans. Geosci. Remote Sensing*, vol. 37, pp. 63–78, Jan. 1999.
- [5] E. G. Njoku, W. J. Wilson, S. H. Yueh, and Y. Rahmat-Samii, "A large-antenna microwave radiometer-scatterometer concept for ocean salinity and soil moisture sensing," *IEEE Trans. Geosci. Remote Sensing*, to be published.
- [6] K. Davis, *Ionospheric Radio*. London, U.K.: Peregrinus, 1990, p. 276.
- [7] J. D. Kraus, *Radio Astronomy*. Powell, OH: Cygnus-Quasar, 1986.
- [8] V. S. Etkin, M. D. Raev, M. G. Bulatov, Yu. A. Militky, A. V. Smirnov, V. Yu. Raizer, Yu. A. Trokhimovsky, V. G. Irisov, A. V. Kuzmin, K. Ts. Litovchenko, E. A. Bepalova, E. I. Skvortsov, M. N. Pospelov, and A. I. Smirnov, "Radiohydrophysical Aerospace Research of Ocean," Tech. Rep. П-1749, Acad. Sci., Space Res. Inst., Moscow, Russia, 1991.
- [9] M. S. Dzura, V. S. Etkin, A. S. Khrupin, M. N. Pospelov, and M. D. Raev, "Radiometers-polarimeters: Principles of design and applications for sea surface microwave emission polarimetry," in *Proc. IEEE Int. Geoscience and Remote Sensing Symp.*, Houston, TX, 1992.
- [10] S. H. Yueh, W. J. Wilson, F. K. Li, W. B. Ricketts, and S. V. Nghiem, "Polarimetric measurements of sea surface brightness temperatures using an aircraft K-band radiometer," *IEEE Trans. Geosci. Remote Sensing*, vol. 33, pp. 85–92, Jan. 1995.
- [11] S. H. Yueh, W. J. Wilson, S. J. Dinardo, and F. K. Li, "Polarimetric microwave brightness signatures of ocean wind directions," *IEEE Trans. Geosci. Remote Sensing*, vol. 37, pp. 949–959, Mar. 1999.
- [12] C. S. Ruf, C. T. Swift, A. B. Tanner, and D. M. LeVine, "Interferometric synthetic aperture microwave radiometry for the remote sensing of the Earth," *IEEE Trans. Geosci. Remote Sensing*, vol. 26, pp. 597–611, Sept. 1988.
- [13] M. Martin-Neira and J. M. Goutoule, "MIRAS-A two dimensional aperture/synthesis radiometers for soil moisture and ocean salinity observations," *Bull. Eur. Space Agency*, vol. 92, pp. 95–104, 1997.
- [14] D. M. LeVine, A. J. Griffis, C. T. Swift, and T. J. Jackson, "ESTAR: A synthetic aperture microwave radiometer for remote sensing applications," *Proc. IEEE*, vol. 82, pp. 1787–1801, Dec. 1994.
- [15] V. G. Irisov, A. V. Kuzmin, M. N. Pospelov, Yu. G. Trokhimovsky, and V. S. Etkin, "The dependence of sea brightness temperature on surface wind direction and speed. Theory and experiment," in *Proc. IEEE Int. Geoscience and Remote Sensing Symp.*, Espoo, Finland, 1991, pp. 1297–1300.
- [16] S. H. Yueh, R. Kwok, and S. V. Nghiem, "Polarimetric scattering and emission properties of targets with reflection symmetry," *Radio Sci.*, vol. 29, pp. 1409–1420, Nov.–Dec. 1994.
- [17] B. D. Wilson, A. J. Mannucci, and C. D. Edwards, "Subdaily northern hemisphere ionospheric maps using an extensive network of GPS receivers," *Radio Sci.*, vol. 30, pp. 639–648, May–June 1995.
- [18] L. Tsang, "Polarimetric passive remote sensing of random discrete scatterers and rough surfaces," *J. Electromagn. Waves Applicat.*, vol. 5, no. 1, pp. 41–57, 1991.
- [19] S. H. Yueh, "Modelling of wind direction signals in polarimetric sea surface brightness temperatures," *IEEE Trans. Geosci. Remote Sensing*, vol. 35, pp. 1400–1418, Nov. 1997.